Journal of Chromatography, 195 (1980) 1–15
Elsevier Scientific Publishing Company, Amsterdam — Printed in The Netherlands

CHROM. 12,753

COMPARATIVE INVESTIGATION OF RADIOACTIVE SOURCES FOR THE ELECTRON CAPTURE DETECTOR

J. A. AYALA* and W. E. WENTWORTH
Department of Chemistry, University of Houston Central Campus, Houston, TX 77004 (U.S.A.)
and
E. C. M. CHEN
School of Science and Technology, University of Houston at Clear Lake City, Houston, TX 77058 (U.S.A.)

(Received September 28th, 1979)

SUMMARY

The effect of pressure and temperature on the current in electron capture detectors has been experimentally evaluated using both ^{63}Ni and scandium tritide radioactive foils. The data were collected as a function of pulse interval and width. The data reflect the greater range of β particles from a ^{63}Ni source and under normal operating conditions suggest that the ionization region extends over the entire volume of the electron capture detector. On the other hand the ionization caused by β particles from ^{3}H is closer to the radioactive foil and more concentrated. The rate of loss of electrons has also been evaluated from this data and it appears to be greater for ionization by ^{3}H than ^{63}Ni. Furthermore, the addition of traces of oxygen appear to increase the rate of loss of electrons to a greater extent with ^{3}H than with ^{63}Ni.

INTRODUCTION

The high sensitivity and selectivity of the electron capture detector (ECD) have made it a very powerful analytical tool in areas such as medical and drug research, among others. The ECD serves as a source of thermal electrons so it is also possible to use it to study the mechanisms of thermal electron attachment (TEA) to molecules[1,2].

The evident importance of the ECD along with unique operational problems have made this detector the subject of numerous studies[1,3–10]. The objective of the studies on the ECD has been either to optimize its performance, or to pursue a better understanding of its operational theory. The kinetic model for a pulsed ECD[1] has been very helpful to explain the results obtained from the ECD response to electron capturing species. More recently, the development of the technique of atmospheric pressure ionization mass spectrometry (API-MS) has allowed some research groups[11,12] to pursue the identification of the products formed in the ECD. In consideration of the new information on the ECD, Wentworth and Chen[13] have revised the original kinetic model for the ECD[1]. In this revision, Wentworth and

0021-9673/80/0000–0000/$02.25

Chen have removed the original assumption that the positive ion concentration remains constant at long pulse intervals within the ECD cell.

Traditionally, radioactive materials have been used as a source of ionizing radiation in the ECD. Several particle emitters have been examined[14,15], and very recently Dwight *et al.*[16] have reported an ^{55}Fe source of high-energy Auger electrons. However, the radioactive sources of the ECD are practically limited to ^{3}H and ^{63}Ni. In general, ^{3}H is preferred on the basis of high specific activities, and lower β^--particle energies but it has a temperature limit of *ca.* 200°C, or 325°C with Sc^3H_3. The ^{63}Ni can withstand temperatures of *ca.* 400°C.

We have attempted in the present work a comparative study of the performance of the ECD with both the scandium tritide and the ^{63}Ni sources. This investigation will presumably shed more light towards understanding the behavior of the ECD. The results are analyzed through the revised kinetic model of Wentworth and Chen. The research includes the pressure and temperature effects, and the effects of the presence of oxygen within the ECD cell.

EXPERIMENTAL

A cylindrical geometry[4] was used for the detector cell. It was made of 316 stainless steel with a radius of 0.7 cm and length of 1.3 cm for the ^{63}Ni detector, and 2.1 cm for the Sc^3H_3 detector in the actual reaction chamber. The detector was sealed with a gold ring, and provided with a TFE insulated collecting electrode. The radioactive sources were: (a) a 15 mCi ^{63}Ni plated platinum foil which completely covered the cell wall, and (b) a 150 mCi Sc^3H_3 foil, 1 cm wide and 2.8 cm long. The following gases were used as thermalizing mixtures: (a) argon + 10% methane from Linde with an oxygen content > 5 ppm; (b) argon + 10% methane from Linde with 5 ppm of oxygen concentration; (c) argon + 10% methane from Big-Three with *ca.* 5 ppm of oxygen content; (d) argon oxygen-free grade from Linde (*ca.* 0.5 ppm oxygen), plus 10% methane UHP from Matheson (East Rutherford, NJ, U.S.A.) (*ca.* 0.5 ppm oxygen). All gases were passed through a 5A molecular sieve trap before entering the ECD. The flow-rate was maintained constant at 150 ml min^{-1} (STP).

A pressure gauge with a 2 atm (30 p.s.i.g.) range was adapted to the detector outlet. The pressure was varied up to a maximum reading of 1.2 atm (17 p.s.i.g.) on the gauge. The variation of the pressure was accomplished by restricting the flow with a needle valve. The temperature was varied from 300–350°C to 25°C. The ECD was covered with asbestos tape and mounted in an aluminum block. Two cartridge heaters connected to a variable transformer were used to heat the aluminum block, and therefore the detector. A mercury thermometer with a range from 0 to 400°C with 1°C divisions was used to measure the temperature of the detector. The thermometer was immersed in the aluminum block and was kept as close as physically possible to the detector cell.

Data of total electrons within the ECD as a function of time, temperature and pressure were obtained. The pulsed mode of operation was used throughout the entire set of experiments. A Datapulse 102 square wave generator was used to pulse the ECD. The potential was —40 V, a pulse width (t_w) between 2 and 4 μsec was used so as to achieve full collection of free electrons; the pulse period (t_p) was

varied from *ca.* 10 to 10,000 μsec. The current produced was measured by means of a Cary 31 vibrating reed electrometer connected to a Houston Instruments single-pen, strip chart recorder. The sensitivity of the electrometer and the recorder were set so as to keep the signal on scale. Typical values were 0.3 or 1 V in the electrometer. For the recorder the sensitivity was set between 1 and 10 mV by means of a variable pot, but unfortunately its absolute value was not measured at the time of the experiments.

KINETIC MODEL

A kinetic model for the reaction occurring in an ECD was presented several years ago[1,2]. At that time the mathematical analysis of the kinetic model was simplified by making certain assumptions. In particular the positive ion concentration was assumed to be in excess and constant during the capturing process. This reduced second order rate expressions to first order, thus making the solution to the differential equations quite amenable. However, in a recent publication Wentworth and Chen[13] have solved the differential equations rigorously using numerical integration and repeating the integration over sufficient pulse periods to attain steady state conditions. In this analysis electron concentration was reduced to zero at the end of each pulse period to simulate the removal of electrons by the applied field. Simultaneously, only a fraction (f) of the positive ion was removed which also could be due to the applied field or could account for diffusion to the walls of the detector. In any event the positive ion concentration did not stay constant and generally decreased as the electron concentration decreased. Consequently, the differential equations must be solved considering the concentration of positive ions as a variable. If we let b represent the concentration of electrons when no capturing species are present, the rate expression for b is given by

$$\frac{d[b]}{dt} = k_p R_\beta - k_D' [\oplus_0] [b] \tag{1}$$

where $[\oplus_0]$ is the concentration of ions when no capturing species is present, $k_p R_\beta$ is the rate of production of electrons and positive ions as a result of the rate at which β particles are emitted from the radioactive foil, and k_D' is the second order recombination rate constant.

Eqn. 1 is integrated over the pulse period at which time the electron concentration is set equal to zero and a fraction f of the positives are removed. This process is repeated until there is no change in the final integrated values for b and $[\oplus_0]$. Numerous integrations have been made for different rate constants, mechanisms, pulse intervals and concentration of capturing species. In all such integrations it was noted that the positive ion concentration was related to the electron concentration by the simple expression:

$$f = \frac{[b]}{[\oplus_0]} \quad \text{or} \quad [\oplus_0] = \frac{[b]}{f} \tag{2}$$

Since only a fraction f of the positive ions $[\oplus_0]$ is removed by a single pulse, it can be concluded that the number of electrons removed at the end of the pulse period will

equal the number of positive species removed from the ECD cell. Substituting eqn. 2 into eqn. 1 gives

$$\frac{d[b]}{dt} = k_p R_\beta - \frac{k'_D}{f}[b]^2 \tag{3}$$

The constants in eqn. 3 can be evaluated in a manner analogous to that carried out previously[1] measuring $[b]$ as a function of pulse interval, t_p. The initial slope of this graph where $t_p \approx 0$, is given by

$$\left(\frac{d[b]}{dt}\right)_{t_p \to 0} = k_p R_\beta \tag{4}$$

The limiting value of $[b]$ at long pulse intervals, $[b]^\infty$, has a slope of zero and

$$\left(\frac{d[b]}{dt}\right)_{t_p \to \infty} = 0 = k_p R_\beta - \frac{k'_D}{f}([b]^\infty)^2$$

and

$$\frac{k'_D}{f} = \frac{k_p R_\beta}{([b]^\infty)^2} \tag{5}$$

Eqns. 4 and 5 were used to evaluate $k_p R_\beta$ and k'_D/f as given in the following results.

RESULTS AND DISCUSSION

Electrons collected versus pulse period

Experimentally in the operation of an ECD we do not measure the electron concentration directly. The measured quantity is an average current, I, as a result of the electrons collected at the duration of each pulse period, t_p. The number of free electrons produced at the end of each pulse period N_{e^-} is simply $(t_p \cdot I)$. If the volume in which the reaction occurs (V_r) were known, the concentration of electrons could then be calculated, $[b] = N_{e^-}/V_r$. Of course the electrons are not homogeneously distributed throughout the cell, so at best we could calculate only some average concentration. This point will be considered in more detail later in the discussion.

The results of this study are presented in Figs. 1–4 where the relative number of electrons as a function of pulse period is shown. Different conditions of pressure, temperature, and oxygen concentration are shown for both ^{63}Ni and Sc^3H_3 β^- sources. Note in Fig. 1 that for ^{63}Ni, increasing pressure at 286°C causes an increase in number of electrons at long pulse intervals, $N_{e^-}^\infty$, whereas at 25°C there is an increase followed by a decrease. For Sc^3H_3 as shown in Fig. 2, $N_{e^-}^\infty$ decreases with increasing pressure at both 296 and 25°C. However, note that curve c is very close to curve b at 296°C and it appears that it is approaching the reversal shown by b and c at 25°C for ^{63}Ni. These seeming inconsistencies are readily explained in terms of the fundamental constants $k_p R_\beta$ and k'_D/f and the reaction volume. This discussion will follow.

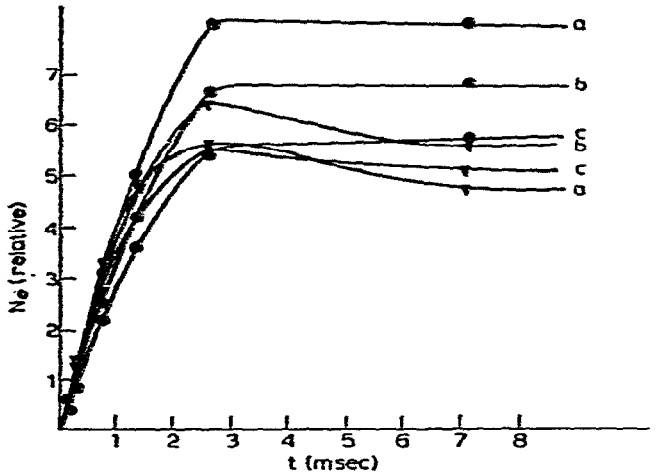

Fig. 1. Electrons collected per pulse *versus* pulse period: ^{63}Ni β^- source, $[O_2]$ *ca.* 0.5 ppm. (a) P = 31.7 p.s.i.a. = 2.2 atm; (b) P = 21.7 p.s.i.a. = 1.5 atm; (c) P = 16.2 p.s.i.a. = 1.1 atm. ●, 286°C; ▼, 25°C.

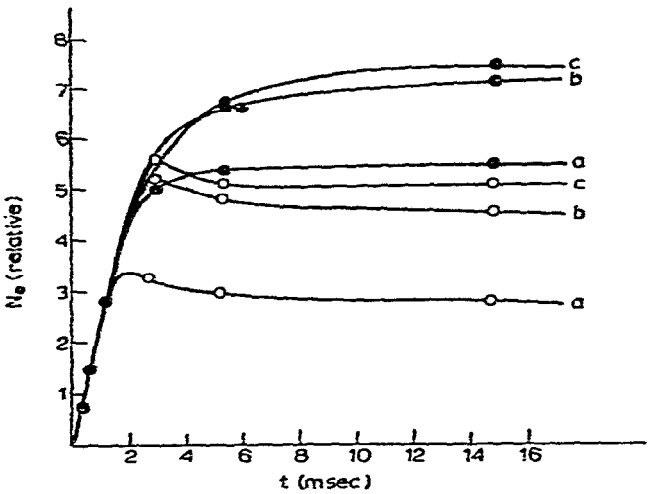

Fig. 2. Electrons collected per pulse *versus* pulse period: Sc^3H_3 β^- source, $[O_2]$ *ca.* 0.5 ppm. (a) P = 31.7 p.s.i.a. = 2.2 atm; (b) P = 21.7 p.s.i.a. = 1.5 atm; (c) P = 16.2 p.s.i.a. = 1.1 atm. ●, 296°C; ○, 25°C.

Similar data at $[O_2] > 5$ ppm are shown in Figs. 3 and 4. For ^{63}Ni there is very little difference at t = 320°C compared with Fig. 1 at 286°C. However, at 25°C, $N_e^{\infty -}$ is nearly independent of pressure and much lower in magnitude. For the Sc^3H_3 the curves are almost unaffected at high temperature whereas the effect on $N_e^{\infty -}$ at 25°C is dramatic. The curve at 25°C and P = 2.2 atm is so low in magnitude that it is barely above the abscissa (not shown in Fig. 4); *i.e.*, $N_e^{\infty -}$ is very pressure dependent at 25°C.

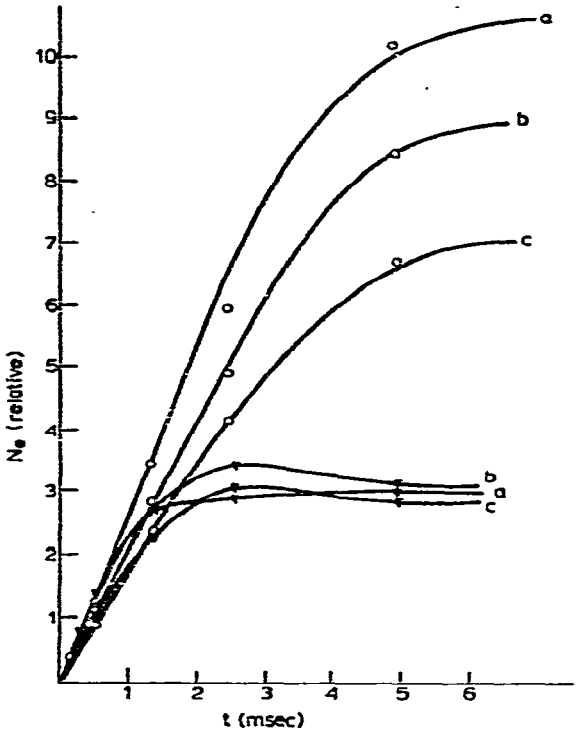

Fig. 3. Electrons collected per pulse *versus* pulse period: ^{63}Ni β^- source, [O_2] *ca.* 5 ppm. (a) P = 31.7 p.s.i.a. = 2.2 atm; (b) P = 21.7 p.s.i.a. = 1.5 atm; (c) P = 16.2 p.s.i.a. = 1.1 atm. ○, 320°C; ▼, 25°C.

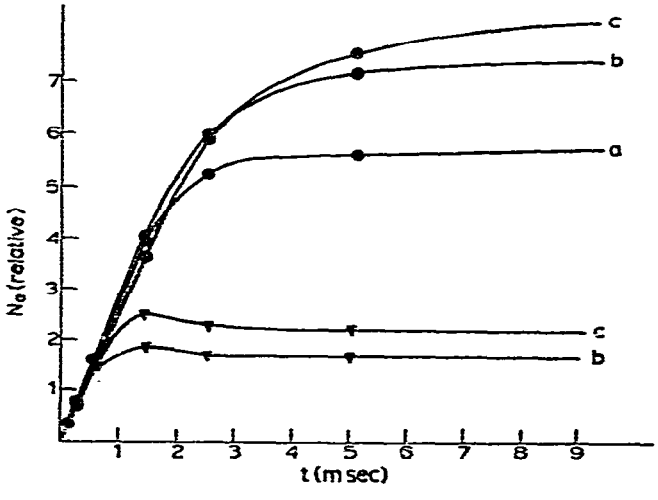

Fig. 4. Electrons collected per pulse *versus* pulse period: Sc^3H_3 β^- source, [O_2] *ca.* 5 ppm. (a) P = 31.7 p.s.i.a. = 2.2 atm; (b) P = 21.7 p.s.i.a. = 1.5 atm; (c) P = 16.2 p.s.i.a. = 1.1 atm. ●, 296°C; ▼, 25°C.

A blow-up of the curves in the region of low pulse intervals is shown in Figs. 5 and 6 for the data when $[O_2]$ *ca.* 0.5 ppm. Note the expected linear relationship between N_{e^-} and t_p. Furthermore, note that there is much greater dependence on temperature and pressure for ^{63}Ni compared to Sc^3H_3. In general, there is an increase in slope with increase in pressure and decrease in temperature.

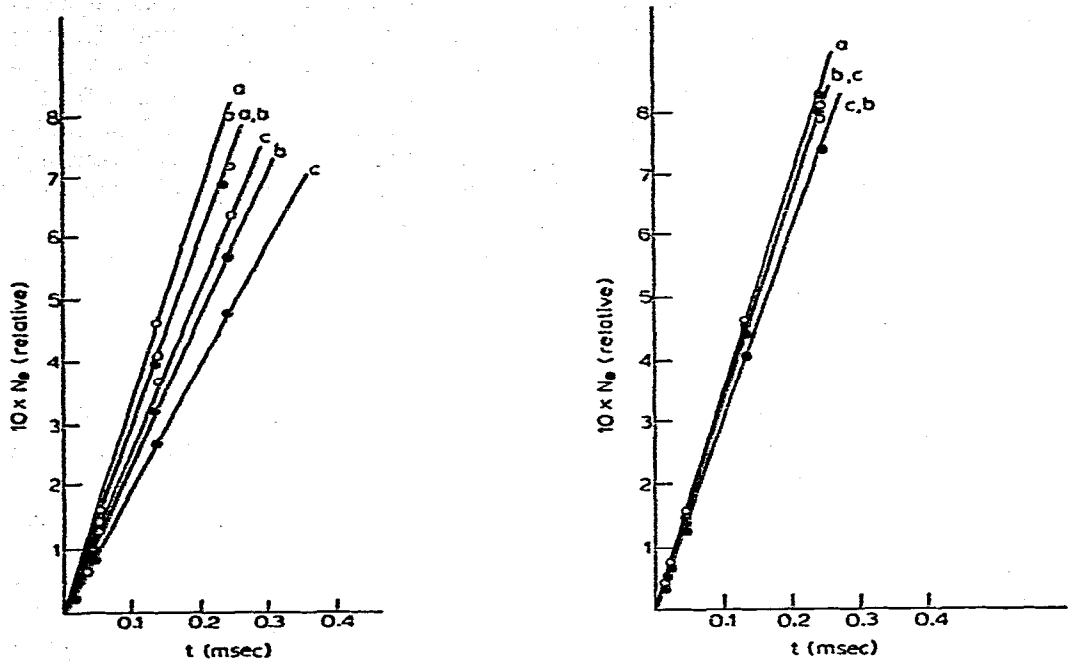

Fig. 5. Electrons collected per pulse at short pulse periods: ^{63}Ni β^- source, $[O_2]$ *ca.* 0.5 ppm. (a) $P = 31.7$ p.s.i.a. $= 2.2$ atm; (b) $P = 21.7$ p.s.i.a. $= 1.5$ atm; (c) $P = 16.2$ p.s.i.a. $= 1.1$ atm. ●, 320°C; ○, 25°C.

Fig. 6. Electrons collected per pulse at short pulse periods: Sc^3H_3 β^- source, $[O_2]$ *ca.* 0.5 ppm. (a) $P = 31.7$ p.s.i.a. $= 2.2$ atm; (b) $P = 21.7$ p.s.i.a. $= 1.5$ atm; (c) $P = 16.2$ p.s.i.a. $= 1.1$ atm. ●, 296°C; ○, 25°C.

Rate of production of thermal electrons

In order to understand more basically the variation in these curves, we will relate them to the fundamental constants k_pR_β and k'_D/f in eqn. 3. The initial slope of the N_{e^-} *vs.* t_p curve is related to the rate constants k_pR_β through eqn. 4 and $[b] = N_{e^-}/V_r$.

$$\left(\frac{d[b]}{dt}\right)_{t_p \to 0} = \frac{1}{V_r} \cdot \left(\frac{dN^{e^-}}{dt}\right)_{t_p \to 0} = k_pR_\beta$$

$$\left(\frac{dN^{e^-}}{dt}\right)_{t_p \to 0} = (k_pR_\beta)\, V_r \qquad (6)$$

Of course since there is a distribution of β^- particles with different energies there will also be a distribution of the ionization in the electron capture cell. The variable [b] would represent some average concentration of the electrons in the reaction volume, V_r.

The rate constant k_pR_β actually depends upon three factors, two of which can be changed experimentally: (a) the flux at which the β^- particles pass through the carrier gas, (b) the ionization efficiency for the β^- particle, and (c) the concentration of the carrier gas. The ionization efficiency will not change unless the composition of the carrier gas is changed and this phenomenon is well understood in radiation chemistry. The flux of β^- particles should remain essentially constant except for the decrease due to contamination of the radioactive surface or a release of the radioactive material to the carrier gas. The most dramatic change in k_pR_β is through the concentration of the carrier gas. At lower pressure this is easily predicted from the ideal gas equation and should be proportional to P/T.

The reaction volume V_r is defined by the range of the β^- particles, which is a function of the density of the medium

$$R^{\max.} = \frac{R_0}{\varrho} \tag{7}$$

where R_0 is the range measured in g cm^{-2} and is assumed to be the same for all materials. R_0 at 1 atm and 25°C can be calculated through the empirical relation given by Katz and Penfold[17]

$$R_0\,(\text{mg cm}^{-2}) = 412\,E_{\max.}^{n} \tag{8}$$

where $n = 1.265 - 0.0954\,(\ln E_{\max.})$, and $E_{\max.}$ is given in MeV. If we again assume the carrier gas obeys the ideal gas equation of state, the density will be proportional to P/T. Consequently, through eqn. 7 the range and hence the reaction volume, providing it is less than the cell volume, is inversely proportional to P/T. Since k_pR_β and possibly V_r are dependent on P/T, we have graphed in detail (dN_{e^-}/dt) at $t_p \to 0$ *vs.* P/T in Fig. 7. Note that the curve for ^{63}Ni continuously increases,

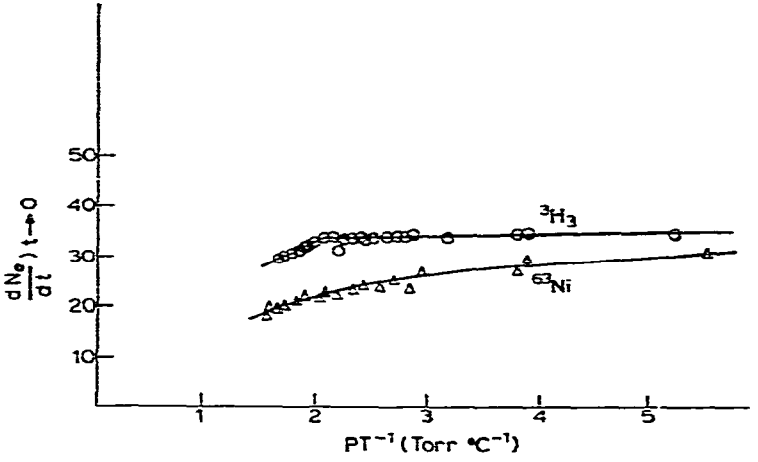

Fig. 7. (dN_{e^-}/dt) at $t_p \to 0$ *versus* P/T.

slowly approaching a maximum. Sc^3H_3, on the other hand, shows an increase up to a maximum value which remains constant at greater P/T values.

These results are understandable if one considers the distribution of β^- particles in the cell as a result of the distribution of the β^- particle energies for Sc^3H_3 and ^{63}Ni. Since the energy distribution for ^3H and ^{63}Ni is available in the literature[18,19] we have estimated the range of distribution (at STP) for both radioactive materials, and the results are shown in Fig. 8. It should be noted that both distributions have not been normalized to the same particle density. However, it is clear from Fig. 8 that the β particles from tritium have a sharper distribution and smaller range than those from ^{63}Ni. It also should be noted that *ca.* 30% of the distribution for ^{63}Ni is within 1.4 cm (the diameter of the detector cell), and that all the radiation from Sc^3H_3 has a range smaller than 1 cm ($R_{max.} = 0.65$ cm STP). Since the range is inversely proportional to the density in a gaseous medium, an increase in P/T will shift the distribution in Fig. 8 towards the left whereas a decrease in P/T will shift it to the right. Consequently, as P/T is increased the maximum range for both sources is decreased and the β particles will be confined to a smaller volume.

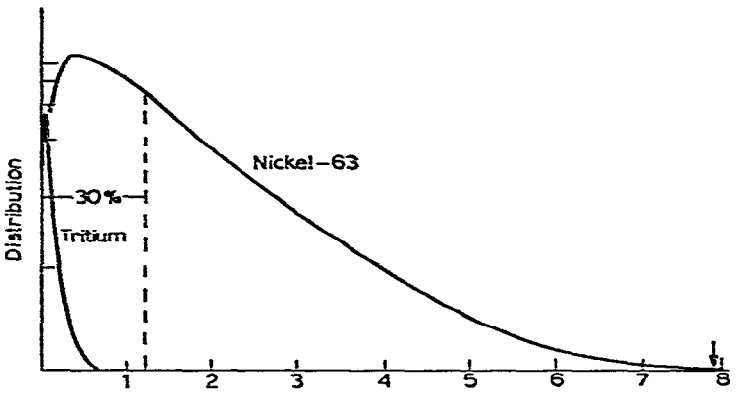

Fig. 8. Distribution of distance travelled by β^- particles.

The graphs in Fig. 8 are in agreement with the experimental results of Simon and Rork[20] who have measured the specific ionization for ^3H and ^{63}Ni as a function of pressure for spherical geometries. They obtained the following results: (a) with a sphere of radius 5.08 cm, the saturation current increases when the pressure is varied from 1 to 760 Torr; furthermore, the saturation current measured for a sphere of 2.54 cm is identical with that in the 5.08 cm cell when twice the pressure is applied; (b) the specific ionization for ^3H drops from *ca.* 10^{-7} A ml^{-1} for a radius of 0.01 cm to *ca.* 10^{-10} A ml^{-1} at 0.4 cm, at 740 Torr. For ^{63}Ni a gradual drop in the specific ionization at 740 Torr from *ca.* 10^{-9} A ml^{-1} at 0.01 cm to *ca.* 10^{-14} A ml^{-1} at 6 cm is observed. The maximum range for tritium is 0.65 cm, and we have estimated a maximum range of 7.9 cm for ^{63}Ni at 760 Torr, which we consider to be in good agreement with the above experimental results.

With the information in Fig. 8 we can account for the behavior in Fig. 7. For

the Sc^3H_3 source (dN_{e^-}/dt) at $t_p \to 0$, is a constant when $P/T > 2$ Torr °C^{-1} and then decreases as P/T decreases. The constant value at higher P/T values is understandable since the β^- particles should be contained in the cell. For example, the range of 0.65 cm at 25°C and 1 atm corresponds to $P/T = 2.55$ Torr °C^{-1} and this is less than the radius of 0.7 cm and the foil width of 1 cm. As P/T increases, the range and reaction volume decrease but k_pR_β increases in a compensating manner so as to make (dN_{e^-}/dt) constant at $t_p \to 0$ (eqn. 6). The decrease at $P/T < 2$ Torr °C^{-1} is understandable since the range of the β^- particles increases to the point where they are lost at the cell walls. At $P/T = 2$ Torr °C^{-1} the range is 0.83 cm and this exceeds the cell radius and is comparable to the foil width of 1 cm. Furthermore, some β^- particles can be emitted from the foil at oblique angles such that they are lost at the curved cell wall or the ends of the cylinder. The decrease observed in Fig. 7 is small since only a small fraction of the β^- distribution for Sc^3H_3, shown in Fig. 8, has the higher ranges. At lower P/T values the distribution will shift sufficiently to higher ranges such that a large fraction of the β particles will exceed 0.83 cm, and consequently (dN_{e^-}/dt) at $t_p \to 0$, should decrease markedly. The decrease in P/T could arise from exceedingly high temperatures or pressures below 1 atm. Since P/T is a measure of gas density, replacing argon (mol.wt. 40) with a lower molecular weight gas such as helium (mol.wt. 4) or nitrogen (mol.wt. 28) would have the effect of lowering P/T. Consequently, for these gases the discontinuity at 2 Torr °C^{-1} in Fig. 7 would be displaced to higher values. For helium it should be at 20 Torr °C^{-1} and for nitrogen 2.85 Torr °C^{-1}. This should be taken into account when designing or using ECDs with these carrier gases.

For ^{63}Ni a constant value for (dN_{e^-}/dt) at $t_p \to 0$, was never attained even up to $P/T = 6$ Torr °C^{-1}. This is expected since at $t = 25$°C and $P = 760$ Torr *ca.* 30% of the radiation has a range lower than 1.2 cm, less than the 1.4 cm diameter of the ECD. This does not mean that only 30% of the ionization will occur within a distance of 1.2 cm. In order to estimate the percentage of ionization within the cell, one must consider the energy for each β^- particle and also include a fraction of the energy of β^- particles with ranges in excess of 1.4 cm since they will cause ionization in passing through the initial 1.4 cm of their path. The calculations are even more complicated in that the angular distribution of the β^- particles as they leave the surface must be taken into account and the loss of β^- particles to the ends of the cylindrical cell. It would appear from Fig. 7 that *ca.* 70% of the ionization has occurred at $P/T = 2.55$ Torr °C^{-1} and 83% at $P/T = 6$ Torr °C^{-1}. Presumably the curve will attain a constant value at much larger P/T values, in a manner similar to that for Sc^3H_3. For Sc^3H_3 at $P/T < 2$ Torr °C^{-1} and for ^{63}Ni the constant k_pR_β is increasing in accord with (dN_{e^-}/dt) at $t_p \to 0$, and eqn. 6. The reaction volume is constant since it is defined by the cell volume in this region.

The limiting value for (dN_{e^-}/dt) at $t_p \to 0$, at high P/T values can be estimated from the following equation:

$$\lim_{(P/T)\to\infty} \left(\frac{dN_{e^-}}{dt}\right)_{t_p\to 0} = \frac{FR_\beta \bar{E}_\beta C}{W} \tag{9}$$

where R_β is the activity of the radioactive foil in curies; F is the fraction of the β^- particles which enter the ionization region of the ECD; $\bar{E}_\beta$ is the average energy of

the β^- particles; W is the energy required to produce an ion pair, typically 35 eV per ion pair; and $C = 3.7 \cdot 10^{10}$ disintegrations sec^{-1} $curie^{-1}$. It is difficult to obtain a value for F since it is a function of not only the geometry of the detector, but also the self-absorption of the β^- particles within the foil. F is certainly less than 0.5 since at least 1/2 of the β^- particles are emitted in the direction of the metal. Others leaving at oblique angles to the foil must travel through additional solid material leading to greater self-absorption. This is especially severe for ^3H β^- particles which are very soft with an average energy of only 5.5 keV. The β^- particles from ^{63}Ni are also considered soft, but their average energy of 17 keV is considerably larger than for ^3H. Self-absorption for ^{63}Ni is generally less severe than for ^3H if the specific activity of ^{63}Ni is high, and only a thin layer need be deposited on the foil. F can be evaluated experimentally by measuring the limiting value for (dN_{e^-}/dt) at $t_p \rightarrow 0$, since all other terms are known in eqn. 9 for both ^{63}Ni and Sc^3H_3.

In this work only relative values of (dN_{e^-}/dt) at $t_p \rightarrow 0$ were determined experimentally, so it is impossible to evaluate the limiting value on an absolute basis. Unfortunately, the sensitivity of the recorder utilized to measure the ECD response was varied to an unknown setting at the time of the experiment. If we neglect this factor, we can calculate a lower limit to the limiting value for (dN_{e^-}/dt) at $t_p \rightarrow 0$. These values are shown in Table I, along with the calculated value of $(R_\beta \bar{E}_\beta C)/W$. The calculated F values are 0.09 for Sc^3H_3 and 0.27 for ^{63}Ni. Considering our discussion in the previous paragraph, these values seem reasonable. These values of F are also of significance with respect to the model for the ECD presented by Siegel and McKeown[11,21] in which only a small fraction of the electrons produced in the ECD are actually collected by the applied potential. These values of F suggest that it is very likely that all the electrons produced can be collected if short pulse intervals of the order of 30 μsec are used. At longer pulse intervals a significant fraction of the electrons recombine with positive ions, but all of the remaining free electrons should be collected during the applied potential. This conclusion is also supported by the recent experimental results from (a) Takeuchi[22] who has measured a value of $1.7 \cdot 10^{10}$ electrons sec^{-1} for $k_p R_\beta$ in an ECD, which is of the same order of magnitude as the results presented herein; (b) Lovelock and Watson[23] who have concluded that the thermal electron drift velocity, in a 30 V cm^{-1} field applied for 1 μsec, is very similar to that of free unimpeded electrons in argon–methane: they used an ECD with a tritium source; and (c) Grimsrud, *et al.*[12] who have presented both experimental and theoretical arguments in favor of the view that the ECD current is a direct measure of the steady-state electron concentration. They also argue that at

TABLE I

ELECTRON PRODUCTION RATES FROM RADIOACTIVE SOURCES

Source	$\left(\frac{dN_{e^-}}{dt}\right)_{t_p=0}$ *(experimental)*	$\frac{R_\beta \bar{E}_\beta C}{W}$	F
Sc^3H_3	$8 \cdot 10^{10}$ sec^{-1}	$9 \cdot 10^{11}$ sec^{-1}	0.09
^{63}Ni	$8 \cdot 10^{10}$ sec^{-1}	$3 \cdot 10^{11}$ sec^{-1}	0.27

least some of the current measured in the ECD is due to positive ion migration to the electrodes, which is in agreement with the new kinetic model for the ECD[13].

Second-order recombination rate constant

Knowing that $[b] = N_{e^-}/V_r$ we can combine eqns. 5 and 6 to obtain an expression for k_D'/f:

$$\frac{k_D'}{f} = \frac{\left(\frac{dN_{e^-}}{dt}\right)_{t_p=0}(V_r)}{(N_{e^-}^{\infty})^2} \tag{10}$$

If k_D' is truly a second-order rate constant, not dependent on a neutral third body, then we would expect k_D'/f to be constant. The ratio, $R = (dN_{e^-}/dt)$ at $t_p \to 0$, divided by $(N_{e^-}^{\infty})^2$, can be calculated from the initial slope and the limiting value of the N_{e^-} as $t_p \to \infty$. Solving for this ratio

$$R = \frac{\left(\frac{dN_{e^-}}{dt}\right)_{t_p=0}}{(N_{e^-}^{\infty})^2} = \frac{k_D'}{f} \cdot \frac{1}{V_r} \tag{11}$$

we see that it is inversely proportional to the reaction volume V_r. As noted before, for the Sc^3H_3 source at $P/T > 2$ Torr $°C^{-1}$ all of the β^- ionization is contained for the most part within the ECD and the reaction volume is inversely proportional to P/T. Consequently, in this region we would expect a graph of R to be directly proportional to P/T. For Sc^3H_3 in the region $P/T < 2$ Torr $°C^{-1}$ and for ^{63}Ni the reaction volume remains constant as defined by the cell volume and one would expect the ratio R to remain constant, independent of P/T.

Graphs of the ratio R *versus* P/T are shown in Figs. 9 and 10 for ^{63}Ni and Sc^3H_3, respectively. Note that for ^{63}Ni the ratio remains essentially constant, ranging from $1.5 \cdot 10^{-6}$ to $3 \cdot 10^{-6}$ sec^{-1}, in the region up to $P/T = 4$ Torr $°C^{-1}$. A single data point at $P/T = 5.6$ Torr $°C^{-1}$ is considerably higher at $5 \cdot 10^{-6}$ sec^{-1}. For Sc^3H_3 in the region $P/T > 2$ Torr $°C^{-1}$ (Fig. 10), a constant value on the order of

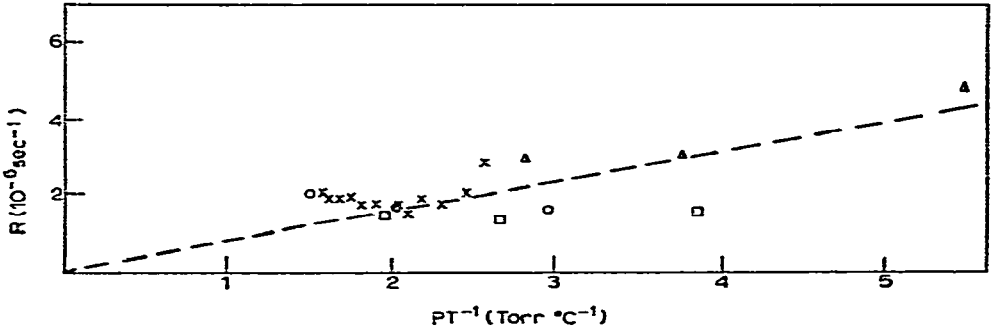

Fig. 9. R *versus* P/T for ^{63}Ni at $[O_2]$ *ca.* 0.5 ppm. ×, 1.1 atm; △, 25°C; □, 147°C; ○, 286°C.

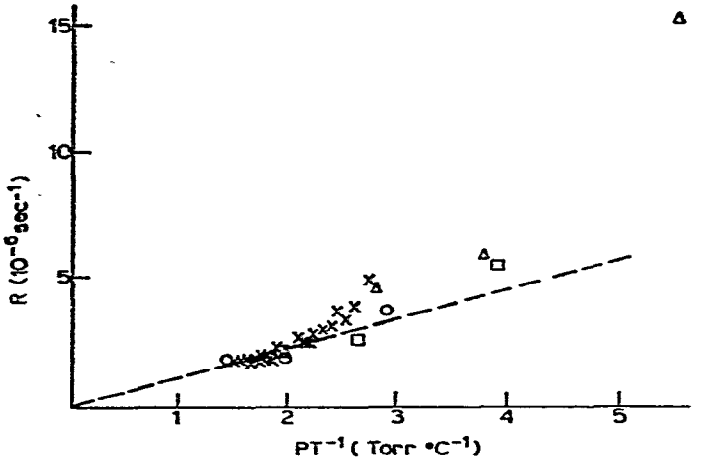

Fig. 10. *R versus P/T* for Sc^3H_3 at $[O_2]$ *ca.* 0.5 ppm. ×, 1.1 atm; △, 25°C; □, 147°C; ○, 296°C.

$2 \cdot 10^{-6}$ sec^{-1} is observed. This value is consistent with the value observed for ^{63}Ni in Fig. 9. On the other hand, in the region $P/T > 2$ Torr $°C^{-1}$, the ratio increases, as we would expect, due to a decrease in reaction volume. However, the increase is greater than one would predict from eqn. 10, as shown by the deviation from the dashed line. The greatest deviation occurs for data points at the lowest temperature (25°C), suggesting a higher order dependence on $1/T$. This would well be due to trace amounts of O_2 in the carrier gas, as will be discussed shortly. The carrier gas used for the data in Figs. 9 and 10 contains *ca.* 0.5 ppm O_2.

The limiting value of R for both ^{63}Ni and Sc^3H_3 is *ca.* $2 \cdot 10^{-6}$ sec^{-1}. Since the reaction volume is defined by the cell volume of 2 ml for ^{63}Ni and 3.2 ml for Sc^3H_3, we can calculate k'_D/f from eqn. 10 to be $4 \cdot 10^{-6}$ and $6.4 \cdot 10^{-6}$, respectively. From a previous study[13], f is typically 0.02–0.05 so k'_D would be estimated as $0.8 \cdot 10^{-7}$–$2 \cdot 10^{-7}$ ml sec^{-1} for ^{63}Ni, and $1.3 \cdot 10^{-7}$–$3.2 \cdot 10^{-7}$ ml sec^{-1} for Sc^3H_3. This estimate for k'_D in the mixture argon–methane (9:1) is in reasonable agreement with the values for the ion–electron recombination coefficient reported for different gases at low pressures, which range between 10^{-6} and 10^{-7} ml sec^{-1} (ref. 24). The value quoted for argon in ref. 24 is $6.7 \cdot 10^{-7}$ ml sec^{-1}, which suggests that the value for f could be higher than the one we have utilized to estimate k'_D.

Effect of oxygen

The effect of O_2 at a concentration greater than 5 ppm on N_{e^-} is shown in Figs. 3 and 4. Recall that the effect was significant for both β^- sources but dramatic for Sc^3H_3 at low temperatures and high pressures. Similar data were obtained for the mixture argon–methane (9:1) containing *ca.* 5 ppm O_2, and an analysis using (dN_{e^-}/dt) at $t_p \rightarrow 0$ and N_{e^-} was performed as described earlier. As somewhat expected, the presence of O_2 has little effect on the initial slopes, (dN_{e^-}/dt) at $t_p \rightarrow 0$, suggesting that $k_p R_\beta$ is unaffected by O_2 even when $[O_2] > 5$ ppm. For the carrier gas containing *ca.* 5 ppm O_2 the presence of O_2 had little effect on the ^{63}Ni source but a dramatic effect on the Sc^3H_3 source. This is shown in Figs. 11 and 12 for

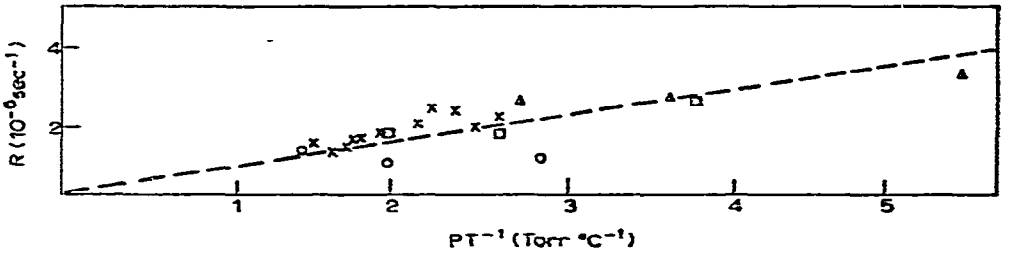

Fig. 11. *R versus P/T* for ^{63}Ni at $[O_2]$ *ca.* 5 ppm. ×, 1.1 atm; △, 25°C; □, 147°C; ○, 320°C.

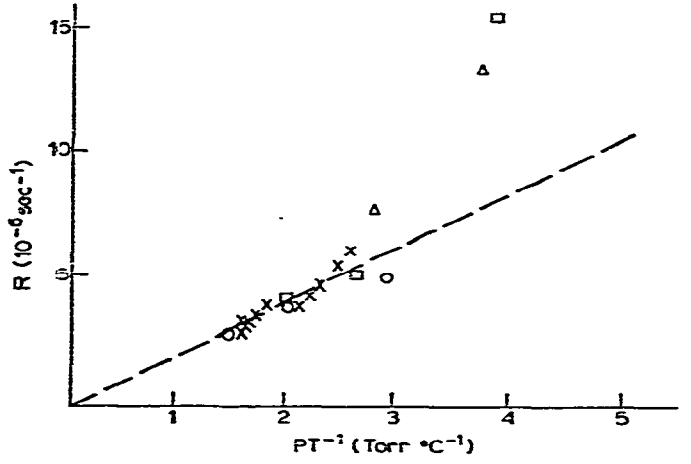

Fig. 12. *R versus P/T* for Sc^3H_3 at $[O_2]$ *ca.* 5 ppm. ×, 1.1 atm; △, 25°C; □, 147°C; ○, 296°C.

^{63}Ni and Sc^3H_3, respectively. Note that Fig. 11 for ^{63}Ni is very similar to Fig. 9 in which $[O_2] = 0.5$ ppm. However, note the large difference between Fig. 12 and Fig. 10 showing the extreme sensitivity of the Sc^3H_3 β^- source for O_2. Most certainly this is due to electron attachment to O_2 and not an effect on k_{ii}/f. The electron attachment to O_2 is especially sensitive to temperature[10] and most certainly this is the reason for the high value of R at large P/T values. Electron attachment to O_2 is also third-body dependent and this also accounts for the sharp increase with increasing P/T. The reason for the relative insensitivity of ^{63}Ni towards O_2 compared to Sc^3H_3 is not completely understood at this time. One possible explanation is that ^{63}Ni does not produce a completely thermal distribution of electrons compared to ^3H since electron attachment to O_2 requires low energy electrons. Further studies need be carried out to clarify this point.

CONCLUSIONS

In summary the following conclusions can be made:

(1) Contaminants such as oxygen should be avoided as much as possible in order to be sure that the ECD theory applies.

(2) The range of the radiation plays an important role in the production of thermal electrons, and in the size of the ECD reaction volume.

(3) It is possible in the case of Sc^3H_3 to obtain 100% ionization efficiency from the β^- particles. In the case of ^{63}Ni, and with the dimensions of the ECD used here, 100% ionization efficiency is only approached at P/T values larger than those at room temperature.

(4) The reaction volume for ^{63}Ni is essentially determined by the cell dimensions. For the tritide source reaction volumes smaller than for ^{63}Ni are estimated.

(5) Practically all the thermal electrons produced can be collected at short pulse intervals.

(6) The loss of electrons appears to be through electron–positive ion recombination.

(7) The second-order recombination rate constant appears to remain essentially constant for both ^{63}Ni and Sc^3H_3, at $P/T < 2$ Torr $°C^{-1}$, provided the reaction volume remains constant.

(8) An ECD using a Sc^3H_3 foil is much more sensitive to O_2 contamination than a ^{63}Ni foil.

ACKNOWLEDGEMENT

This work was supported by a grant from the Robert A. Welch Foundation, E095.

REFERENCES

1 W. E. Wentworth, E. Chen and J. E. Lovelock, *J. Phys. Chem.*, 70 (1966) 445.
2 W. E. Wentworth and J. C. Steelhammer, *Advan. Chem. Ser.*, 82 (1968) 74.
3 W. E. Wentworth and E. Chen, *J. Gas Chromatogr.*, 5 (1967) 170.
4 A. Zlatkis and D. C. Fenimore, *Rev. Anal. Chem.*, 2 (1975) 317.
5 W. A. Aue and S. Kapila, *J. Chromatogr. Sci.*, 11 (1973) 255.
6 R. J. Maggs, P. L. Joynes, A. J. Davies and J. E. Lovelock, *Anal. Chem.*, 43 (1971) 1966.
7 C. Gosselin, G. B. Martin and A. Boudreau, *J. Chromatogr.*, 90 (1974) 113.
8 E. D. Pellizzari, *J. Chromatogr.*, 98 (1974) 323.
9 J. E. Lovelock, *J. Chromatogr.*, 99 (1974) 3.
10 H. J. Van de Wiel and P. Tommassen, *J. Chromatogr.*, 71 (1972) 1.
11 M. W. Siegel and M. C. McKeown, *J. Chromatogr.*, 122 (1976) 397.
12 E. P. Grimsrud, S. H. Kim and P. L. Gobby, *Anal. Chem.*, 51 (1979) 223.
13 W. E. Wentworth and E. C. M. Chen, *J. Chromatogr.*, 186 (1979) 99.
14 G. R. Shoemake, D. C. Fenimore and A. Zlatkis, *J. Gas Chromatogr.*, 3 (1965) 285.
15 P. G. Simmonds, D. C. Fenimore, B. C. Pettit, J. E. Lovelock and A. Zlatkis, *Anal. Chem.*, 39 (1967) 1428.
16 D. J. Dwight, E. A. Lorch and J. E. Lovelock, *J. Chromatogr.*, 116 (1976) 257.
17 L. Katz and A. S. Penfold, *Rev. Mod. Phys.*, 24 (1952) 28.
18 L. Slack and K. Way, *U.S. Atomic Energy Commission*, 1959.
19 I. L. Preiss, R. W. Fink and B. L. Robinson, *J. Inorg. Nucl. Chem.*, 4 (1957) 233.
20 F. N. Simon and G. D. Rork, *Rev. Sci. Instrum.*, 47 (1976) 74.
21 M. W. Siegel and M. C. McKeown, *Res./Develop.*, July (1977) 101.
22 M. Takeuchi, *Nippon Kagaku Kaishi*, 10 (1976) 1565.
23 J. E. Lovelock and A. J. Watson, *J. Chromatogr.*, 158 (1978) 123.
24 E. W. McDaniel, *Collision Phenomena in Ionized Gases*, Wiley, New York, 1964, Ch. 12, p. 610.